Article type: Communications

A Highly Stretchable and Fatigue-free Transparent Electrode Based on an In-plane Buckled Au Nanotrough Network

Siya Huang, Yuan Liu, Chuan Fei Guo, and Zhifeng Ren**

Dr. S. Huang, Ms. Y. Liu, Prof. Z. Ren

Department of Physics and TcSUH, University of Houston, Houston, Texas 77204, USA

Email: zren@uh.edu

Prof. C. F. Guo

Department of Materials Science and Engineering, South University of Science and Technology of China, Shenzhen, Guangdong 518055, China

Email: guocf@sustc.edu.cn

Keywords: flexible transparent electrodes, stretchable, nanotrough, electrospinning, in-plane buckling

Introduction

As an essential part of flexible optoelectronic devices, high performance flexible transparent electrodes (FTEs) are gaining increasing attention from soft electronic industry. The traditional transparent electrodes made by indium tin oxide (ITO) thin films have long been facing challenges of poor flexibility due to its intrinsic brittleness and the low abundance of indium element.[1] In the past decade, numerous candidates have been proposed by researchers as alternatives to ITO, such as graphene,[2-5] carbon nanotube (CNT) films,[2,6-8] conducting polymers,[9,10] metallic thin films,[11,12] and metal nanowire networks.[2,13-17] Among them, metallic materials exhibit the best electrical conductance. However, metallic thin films encounter a problem of limited optical transmittance (T). Though metal nanowire networks show greatly improved optical transparency (*e.g.*, $T > 90\%$ for Ag nanowires (AgNWs)[13,16]), they suffer from large contact resistance caused by the poor junctions between separate nanowires, which cripple their mechanical flexibility especially under large strains. Interconnected metal nanowire networks are able to eliminate junction resistance, showing optimal optoelectronic performance with enhanced mechanical flexibility.[18,19] Wu *et al.* developed a facile method to fabricate a free-standing metallic nanotrough network, which shows impressive optoelectronic performance (sheet resistance R_{sh} ~8 Ω sq^{-1} at T = ~90% for Au nanotroughs) with superior bendability.[19] However, its stretchability is far from satisfaction, exhibiting a limited tensile strain up to 50%.[19] It has been reported that the stretchability of the metal nanotroughs can be improved by fabricating hybrid nanostructures based on metal nanotrough networks combined with two-dimensional materials such as graphene.[20] However, the improvement of stretchability is still quite limited (a maximum tensile strain of 80%) while the optical transmittance is inevitably impaired with additional

graphene films.[20] In addition, very few work has been reported on the mechanical fatigue properties of FTEs under cyclic stretching, which is of great significance for long-term service of FTEs in practical devices.

In this paper, we present an extremely stretchable FTE with competent optoelectronic performance (R_{sh} ~10 Ω sq^{-1} at T = 91%) based on a buckled metal nanotrough network. A particularly designed in-plane sinusoidal buckling structure was introduced into the Au nanotrough network by tuning the geometry parameters of the nanotrough and applying adequate pre-strain to polydimethylsiloxane (PDMS) substrates. The as-obtained wavy networks demonstrate superior stretchability with tensile strain up to 300%. Notably, we show that such in-plane buckled nanotrough network structure is completely fatigue-free, exhibiting no resistance increase upon cyclic stretching at 100% strain for 100,000 cycles, suggesting its great potential as highly stretchable FTEs for soft electronics, such as interactive electronics,[21] epidermal electronics,[22,23] and bio-integrated medical devices.[24]

Results and discussion

The preparation of the buckled Au nanotrough network consists of two steps, the fabrication of a freestanding nanotrough network and the following transfer process. As shown in **Figure 1**, the freestanding polymer nanofiber network was fabricated by electrospinning, followed by electron-beam evaporation of metal films on top as reported.[19] Herein, Au films with a thickness of 100-125 nm were evaporated onto the template. Since Au was uniformly coated on the upper side of the nanofibers, an interconnected Au nanotrough network can be

achieved after removing the polymer template (**Figure S1**). The line width, density and alignment of the Au nanotrough network are determined by the underlying nanofiber template, which can be tuned by adjusting the electrospinning parameters (*e.g.*, concentration of polymer solutions, collection time and configuration of collectors). Then, the freestanding Au nanotrough network was transferred onto a pre-strained PDMS substrate. Before transferring, the PDMS substrate (original length L) was stretched biaxially to a certain length ($L+\Delta L$) to apply a desired pre-strain (ε_{pre}). After transferring, the pre-strained substrate was slowly released. Since PDMS is highly flexible (Young's modulus ~1 MPa), the pre-strained PDMS substrate could recover its original length (L). However, the release of pre-strain would in turn exert a compressive strain on the Au nanotroughs adhered to the substrate surface, leading to formation of buckled wavy microstructures.

The configurations of the nanotrough network before and after the transfer process were studied by scanning electron microscopy (SEM). As shown in **Figure 2**(a), aligned polymer nanofiber webs with an average diameter of ~150 nm can be collected with our particularly designed square Cu frames. After transferring onto a biaxially pre-strained PDMS substrate (ε_{pre} = 50%) and slowly releasing the pre-strain, the nanotroughs snapped into an in-plane buckling configuration (Figure 2(b)). The nanotroughs aligned with the direction of pre-strain form well-defined periodic sinusoidal geometry (Figure 2(c)), while the ones that did not form this configuration are either poorly aligned or much larger in size due to the randomness of electrospinning (indicated by arrows in Figure 2(b)).

Note that the deformation mode of our Au nanotrough network upon release of pre-strain is different from those of CNTs[25] or metallic thin films[26], which opt into formation of

out-of-plane wrinkles upon compression. The out-of-plane deformation would significantly increase the surface roughness of FTEs, which is not desired in thin film devices and may cause severe short circuit failures. In contrast, the wavy microstructures observed in our Au nanotrough networks are an in-plane layout. The topology of our buckled Au nanotroughs was examined by atomic force microscopy (AFM). As shown in Figure 2(d), the heights of different segments of a wavy nanotrough are highly consistent, confirming that the buckling occurs laterally within the plane.

The deformation mode of the Au nanotrough network can be controlled by tuning the diameter of the nanotrough as well as the pore size of the network. Under the same condition, the few Au nanotroughs with comparatively large diameters (d ~850 nm) do not form sinusoidal wavy structures as those with small diameters (d ~200 nm), and some of them even fracture at the bending point (**Figure S2**). As proposed by Ryu *et al.*,[27] the wavelength (λ) and amplitude (A) of the in-plane sinusoidal geometry are determined by the nanowire radius r and the Young's modulus ratio of the Au nanotrough (E_{AuNT}) and the PDMS substrate (E_{PDMS}), as given by the following equations[27]

$$\lambda \approx \frac{12\pi}{5}\left(\frac{E_{AuNT}}{E_{PDMS}}\right)^{1/4} r, \tag{1}$$

$$A \approx \frac{12}{5}\left(\frac{E_{AuNT}}{E_{PDMS}}\right)^{1/4} r\sqrt{\varepsilon_{pre}-\varepsilon_{critical}}, \tag{2}$$

where $\varepsilon_{\mathrm{pre}}$ is the pre-strain, and $\varepsilon_{\mathrm{critical}}$ is the critical pre-strain for buckling, given by

$$\varepsilon_{critical} \approx \frac{3}{10}\left(\frac{E_{PDMS}}{E_{AuNT}}\right)^{1/2}. \tag{3}$$

The Young's modulus of PDMS and Au nanowire are 2.67 MPa (ref. 27) and 70 GPa (ref. 28), respectively, and r is ~50 nm in this case. Accordingly, the theoretical wavelength λ and amplitude A are calculated to be 4.8 μm and 1.52 μm, respectively, in good agreement with our experimental data from AFM ($\lambda_m = 4.23 \pm 0.40$ μm and $A_m = 1.05 \pm 0.08$ μm). In addition, the pore size D of the nanotrough network also affects the deformation mode upon strain release. As shown in **Figure S3**, out-of-plane wrinkles can be observed in the Au nanotrough network with a small pore size (D). This can be attributed to the high density of nanotrough junctions, which severely constrain the in-plane buckling of nanotroughs with boundary restriction. Thus, the nanotrough is forced to deform out-of-plane.

Such an in-plane buckled Au nanotrough network shows extraordinary stretchability with impressive low fatigue. As shown in **Figure 3**(a), the buckled Au nanotrough network (uniaxially 100% pre-strained, $R_0 = 29.4\ \Omega\ sq^{-1}$) can be stretched to 100% with only 6% increase in resistance ($R_{100\%} = 31.1\ \Omega\ sq^{-1}$). When the tensile strain increases to 300%, which is four times the initial length of the buckled Au nanotrough network, R increases only by 6 times ($R_{300\%} = 211.5\ \Omega\ sq^{-1}$). In stark contrast, the as-collected nanotrough network without pre-strain show rapid increase in R upon stretching to strain over 20%, and completely loses its conductance at 110%. The huge difference of stretchability between samples with and without applied pre-strain lies in the fact that the compression-induced buckling topology can release the applied strains via structural relaxation. Accordingly, upon extremely large tensile strain up to 300% the buckled Au nanotrough film can still maintain a practically acceptable sheet resistance. Such a high level of stretchability can survive most practical applications, indicating the great potential of buckled Au nanotrough networks as flexible electrodes for stretchable electronics.

Notably, the buckled Au nanotrough films exhibit no fatigue under cyclic stretching to 100% strain for 100,000 cycles. The fatigue of FTEs is a very important property in light of the practical applications in flexible devices, whereas few FTE materials have been reported to exhibit low fatigue when repeatedly stretched to strains larger than 100%. Cyclic tensile tests were carried out with our buckled Au nanotrough films which were transferred onto uniaxially pre-strained PDMS substrates (ε_{pre} = 100%). Here, R_s indicates the resistance of the nanotrough film under tensile strain and R_r the resistance measured after releasing of strain. As presented in Figure 3(b), both R_s and R_r are consistently stable during 100,000 cycles of stretching to 100% strain, showing negligible decay in its electrical conductance. Due to cold-welding effect which occurs spontaneously during natural relaxing and cyclic stretching,[29] the resistance R_s of the Au nanotrough film even decreases by ~5%. Some fractured Au nanotroughs which broke apart due to the lateral tensile strains during the initial pre-strain releasing process and the subsequent cyclic stretching test may be welded together by localized shifting and re-touching under internal compressive stress, leading to gradual recovery of conductance. For tensile strains up to 120%, R_s increases by only 38% after 100,000 cycles, suggesting its outstanding flexibility and stability over long-term service. In comparison with the mechanical flexibility of state-of-the-art FTE materials reported in the literature (**Table 1**), our buckled Au nanotrough network exhibits superior stretchability with tensile strains up to 300%. Remarkably, we show for the first time that excellent stretching cyclability at high strain level up to 120% for a record number of 100,000 cycles can be achieved in our buckled Au nanotrough based FTEs. Such a highly stretchable and durable flexible electrode can meet the requirements of most practical applications, offering great potential in soft electronic industries.

Besides, the Au nanotrough network shows superior optoelectronic performance. As shown in **Figure 4**(a), the optical transmittance T reaches 91% over a broad wavelength range from 300 to 3000 nm, while the sheet resistance R_{sh} is as low as ~10 Ω sq^{-1}, comparable to the best results in literature.[13,16,31] Such a highly transparent and conductive electrode with unprecedented mechanical flexibility are very promising for next-generation wearable electronics, such as epidermal devices[23] and bio-integrated electronics.[24] As demonstrated in Figure 4(b), the Au nanotrough film is ready to be transferred to human skins without causing any skin irritation. To demonstrate the overall performance of Au nanotrough films as FTEs, a red LED light was connected in series with the film attached on human skin, which went through subsequent severe deformations, such as stretching, compressing and even twisting. As seen in Figure 4(c-e), no detachment or crumbling can be observed in the film and the LED showed consistent luminance during the whole skin deformation process, indicating that there was no significant degradation on its electrical resistance. The excellent conformability and durability of the Au nanotrough film with great ease of transfer enable its wide applications in wearable electronics under demanding practical conditions.

Conclusions

In conclusion, we report on a high-performance FTE based on a buckled Au nanotrough network. By precisely tuning the size of the nanotrough as well as the configuration of the network, in-plane buckled sinusoidal structures were introduced into the metal nanotrough network on pre-strained PDMS substrates. In such a particularly designed periodic wavy layout, the buckled Au nanotrough network presents extraordinary mechanical flexibility

with modest resistance increase even under extremely large tensile strain up to 300%. Moreover, the buckled Au nanotrough network is completely free of fatigue, exhibiting stable electrical conductance during 100,000 cycles of tensile tests at strain up to 100%. We further demonstrate that our Au nanotrough network can be readily applied to human skin as flexible electrodes for wearable devices under severe deformations, indicating its great compatibility and durability in practical applications. Combined with its excellent optoelectronic performance (R_{sh} ~10 Ω sq^{-1} at T = 91%), the buckled nanotrough network offers enormous potential as stretchable FTEs in flexible electronics.

Experimental Section

Fabrication of polymer nanofiber template: The polymer nanofiber network was prepared by electrospinning. Polyvinylpyrrolidone (PVP, M_w=1,300,000 Sigma-Aldrich) and poly(vinyl butyral-co-vinyl alcohol-co-vinyl acetate) (M_w=50,000-80,000, Sigma-Aldrich) were chosen as the raw materials for two kinds of polymer nanofibers. PVP powders were dissolved in a mixed solvent of ethanol and deionized water in a weight ratio of 2:6:11. Poly(vinyl butyral-co-vinyl alcohol-co-vinyl acetate) powders were dissolved in pure ethanol at a weight ratio of 12.6%. The solution was stirred at room temperature until formation of a clear homogeneous sol, and then pumped into a syringe which was connected to a high-voltage power supply. Under a high voltage of 12 kV and a working distance of 20 cm, the electrospun nanofiber network can be collected with our home-made square copper frames, which were grounded during electrospinning.

Fabrication of interconnected Au nanotrough networks: A layer of Au in thickness of 100-125 nm was deposited onto the freestanding polymer nanofiber template by electron-beam evaporation (Thermionics, USA) at a deposition rate of ~1 Å/s. Samples were then transferred to the target substrate and rinsed in ethanol to remove the polymer template.

Sample characterizations: To measure the electrical and optical properties of Au nanotrough films, samples were transferred onto clean glass substrates. The sheet resistance was tested by a two-probe method. The specular transmittance was measured with a Cary 5000 UV-Vis-NIR 293 Spectrophotometer (Agilent Technologies, USA) over a wavelength range from 300 to 3000 nm. The samples were transferred onto pre-strained as-cured PDMS substrates (Dow Corning, USA) with a drop of PDMS base on top to reduce the surface friction between nanotroughs and the underlying substrate. The buckled samples were observed under both scanning electron microscopy (SEM, Leo 1525 FEG, Zeiss, USA) and atomic force microscopy (AFM, Veeco Dimensions 3000, Veeco, USA). In our experiment, two kinds of pre-strains, i.e., biaxial (50%) and uniaxial (100%) tensile strains, were applied to the PDMS substrate, respectively. In the case of biaxial pre-strains, the Au nanotrough network can form sinusoidal structures in both orthogonal directions, enabling the as-obtained network stretchability in an omnidirectional way. High level of uniaxial pre-strains endows the Au nanotrough network with larger stretchability along its pre-strain direction, while impairing its conductivity in the perpendicular direction. Thus, biaxial

pre-strains were applied to study the formation mechanism of the wavy pattern, while large uniaxial pre-strains were used for tensile tests.

Demonstration of skin-like electrodes: A free-standing Au nanotrough film was transferred directly onto the surface of human skin. Copper conductive adhesive tapes were attached to two ends of the film, connected in series to a red LED light (forward voltage ~2V).

Supporting Information

Supporting Information is available from the Wiley Online Library or from the author.

Acknowledgements

S.H. and Y.L. contributed equally to this work. The work is financially supported by DOE under a contract DE-SC0010831.

References

[1] O. Inganäs, *Nat. Photonics* **2011**, *5*, 201.

[2] D. S. Hecht, L. Hu, G. Irvin, *Adv. Mater.* **2011**, *23*, 1482.

[3] K. S. Kim, Y. Zhao, H. Jang, S. Y. Lee, J. M. Kim, K.S. Kim, J.-H. Ahn, P. Kim, J.-Y. Choi, B. H. Hong, *Nature* **2009**, *457*, 706.

[4] S. Bae, H. Kim, Y. Lee, X. Xu, J.-S. Park, Y. Zheng, J. Balakrishnan, T. Lei, H. R. Kim, Y. I. Song, Y.-J. Kim, K. S. Kim, B. Özyilmaz, J.-H. Ahn, B. H. Hong, S. Iijima, *Nat. Nanotechnol.* **2010**, *5*, 574.

[5] X. Li, Y. Zhu, W. Cai, M. Borysiak, B. Han, D. Chen, R. D. Piner, L. Colombo, R. S. Ruoff, *Nano Lett.* **2009**, *9*, 4359.

[6] C. Feng, K. Liu, J.-S. Wu, L. Liu, J.-S. Cheng, Y. Zhang, Y. Sun, Q. Li, S. Fan, K. Jiang, *Adv. Funct. Mater.***2010**, *20*, 885.

[7] Z. Wu, Z. Chen, X. Du, J. M. Logan, J. Sippel, M. Nikolou, K. Kamaras, J. R. Reynolds, D. B. Tanner, A. F. Hebard, A. G. Rinzler, *Science* **2004**, *305*, 1273.

[8] D. Zhang, K. Ryu, X. Liu, E. Polikarpov, J. Ly, M. E. Tompson, C. Zhou, *Nano Lett.***2006**, *6*, 1880.

[9] M. Vosgueritchian, D. J. Lipomi, Z. Bao, *Adv. Funct. Mater.* **2012**, *22*, 421.

[10] S. I. Na, S. S. Kim, J. Jo, D. Y. Kim, *Adv. Mater.* **2008**, *20*, 4061.

[11] S. Schubert, J. Meiss, L. Müller-Meskamp, K. Leo, *Adv. Energy Mater.* **2013**, *3*, 438.

[12] W. Wang, M. Song, T.-S. Bae, Y. H. Park, Y.-C. Kang, S.-G. Lee, S.-Y. Kim, D. H. Kim, S. Lee, G. Min, G.-H. Lee, J.-W. Kang, J. Yun. *Adv. Funct. Mater.* **2014**, *24*, 1551.

[13] M. Song, D. S. You, K. Lim, S. Park, S. Jung, C. S. Kim, D.-H. Kim, D.-G. Kim, J.-K. Kim, J. Park, Y.-C. Kang, J. Heo, S.-H. Jin, J. H. Park, J.-W. Kang, *Adv. Funct. Mater.* **2013**, *23*, 4177.

[14] A. R. Rathmell, S. M. Bergin, Y. L. Hua, Z. Y. Li, B. J. Wiley, *Adv. Mater.* **2010**, *22*, 3558.

[15] S. De, T. M. Higgins, P. E. Lyons, E. M. Doherty, P. N. Nirmalraj, W. J. Blau, J. J. Boland, J. N. Coleman, *ACS Nano* **2009**, *3*, 1767.

[16] P. Lee, J. Lee, H. Lee, J. Yeo, S. Hong, K. H. Nam, D. Lee, S. S. Lee, S. H. Ko, *Adv. Mater.* **2012**, *24*, 3326.

[17] D. Zhang, R. Wang, M. Wen, D. Weng, X. Cui, J. Sun, H. Li, and Y. Lu, *J. Am. Chem. Soc.* **2012**, *134*, 14283.

[18] C. F. Guo, T. Sun, Q. Liu, Z. Suo, Z. Ren, *Nat. Commun.* **2014**, *5*, 3121.

[19] H. Wu, D. Kong, Z. Ruan, P.-C. Hsu, S. Wang, Z. Yu, T. J. Carney, L. Hu, S. Fan, Y. Cui, *Nat. Nanotechnol.* **2013**, *8*, 421.

[20] B. W. An, B. G. Hyun, S.-Y. Kim, M. Kim, M.-S. Lee, K. Lee, J. B. Koo, H. Y. Chu, B.-S. Bae, and J.-U. Park, *Nano Lett.* **2014**, *14*, 6322.

[21] M. C. LeMieux, Z. Bao, *Nat. Nanotechnol.***2008**, *3*, 585.

[22] D. J. Lipomi, M. Vosgueritchian, B. C-K. Tee, S. L. Hellstrom, J. A. Lee, C. H. Fox, Z. Bao, *Nat. Nanotechnol.* **2011**, *6*, 788.

[23] D.-H. Kim, N. Lu, R. Ma, Y.-S. Kim, R.-H. Kim, S. Wang, J. Wu, S. M. Won, H. Tao, A. Islam, K. J. Yu, T. Kim, R. Chowdhury, M. Ying, L. Xu, M. Li, H.-J. Chung, H. Keum, M. McCormick, P. Liu, Y.-W. Zhang, F. G. Omenetto, Y. Huang, T. Coleman, J. A. Rogers, *Science* **2011**, *333*, 838.

[24] D.-H. Kim, J. Viventi, J. J. Amsden, J. Xiao, L.Vigeland, Y.-S. Kim, J. A. Blanco, B. Panilaitis, E. S. Frechette, D. Contreras, D. L. Kaplan, F.G. Omenetto, Y. Huang, K.-C. Hwang, M. R. Zakin, B. Litt, J. A. Rogers, *Nat. Mater.* **2010**, *9*, 511.

[25] D.-Y. Khang, J. Xiao, C. Kocabas, S. MacLaren, T. Banks, H. Jiang, Y. Y. Huang, J. A. Rogers, *Nano Lett.* **2008**, *8*, 124.

[26] N. Bowden, S. Brittain, A. G. Evans, J. W. Hutchinson, G. M. Whitesides, *Nature* **1998**, *393*,146.

[27] S. Y. Ryu, J. Xiao, W. I. Park, K. S. Son, Y. Y. Huang, U. Paik, J. A. Rogers, *Nano Lett.* **2009**, *9*, 3214.

[28] B. Wu, A. Heidelberg, J. J. Boland, *Nat. Mater.* **2005**, *4*, 525.

[29] C. F. Guo, Y. Lan, T. Sun, Z. Ren, *Nano Energy* **2014**, *8*, 110.

[30] J. Lee, P. Lee, H. B. Lee, S. Hong, I. Lee, J. Yeo, S. S. Lee, T.-S. Kim, D. Lee, S. H. Ko, *Adv. Funct. Mater.* **2013**, *23*, 4171.

[31] J. Liang, L. Li, K. Tong, Z. Ren, W. Hu, X. Niu, Y. Chen, Q. Pei, *ACS Nano* **2014**, *8*, 1590.

[32] P. Lee, J. Ham, J. Lee, S. Hong, S. Han, Y. D. Suh, S. E. Lee, J. Yeo, S. S. Lee, D. Lee, S. H. Ko, *Adv. Funct. Mater.* **2014**, *24*, 5671.

[33] C. F. Guo, Q. Liu, G. Wang, Y. Wang, Z. Shi, Z. Suo, C.-W. Chu, Z. Ren, *Proc. Natl. Acad. Sci.* **2015**, *112*, 12332.

[34] Y. Jin, S. Hwang, H. Ha, H. Park, S.-W. Kang, S. Hyun, S. Jeon, S.-H. Jeong, *Adv. Electron. Mater.* **2016**, *2*, 1500302.

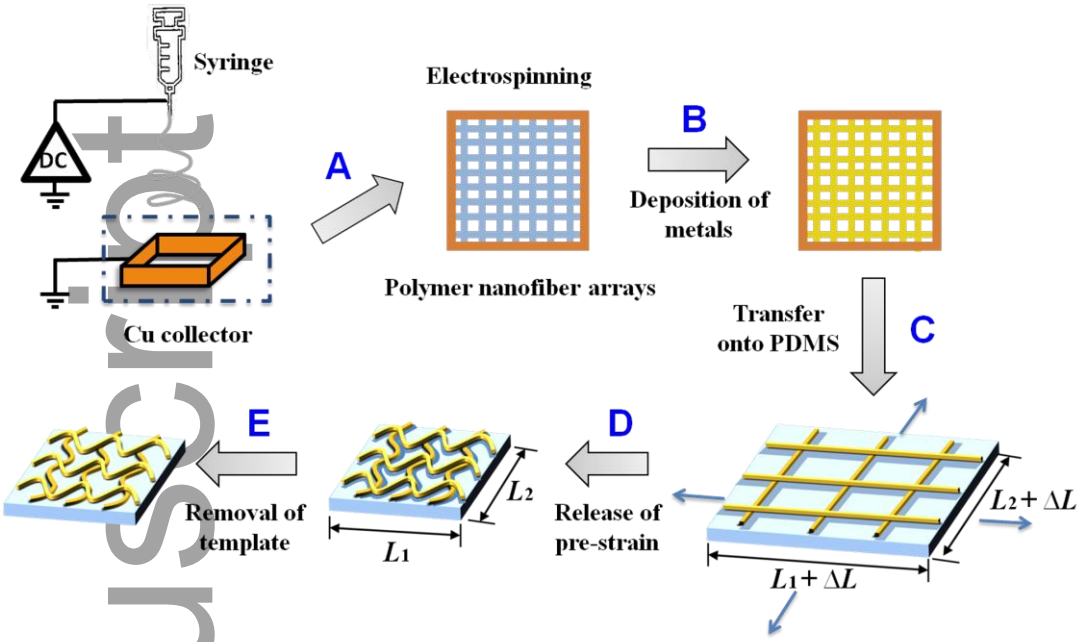

Figure 1. Schematic of the fabrication process of buckled Au nanotrough networks.

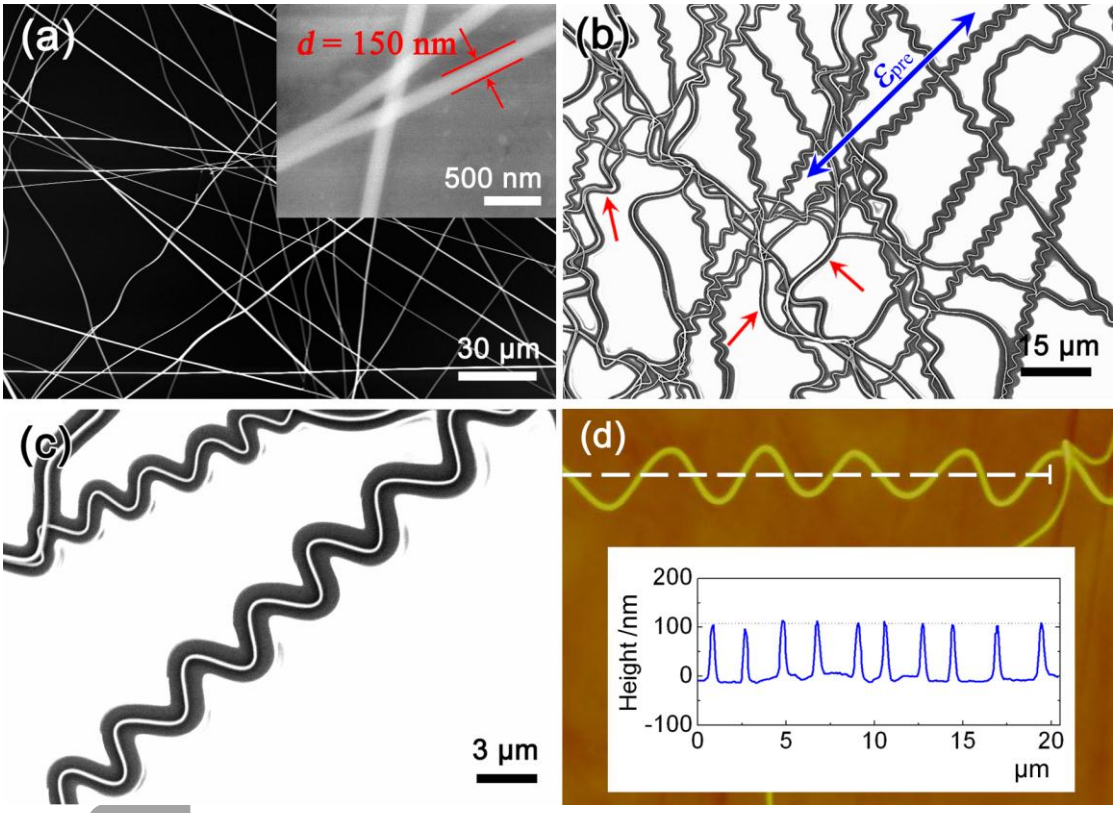

Figure 2. (a) SEM image of a freestanding electrospun PVP nanofiber network. Inset is a magnified SEM image of the nanofibers, showing an average diameter of ~150 nm. (b) SEM image of a buckled Au nanotrough network on PDMS after releasing the pre-strain. The nanotroughs in large diameters (indicated by red arrows) do not form well-defined sinusoidal patterns. (c) Magnified image of buckled Au nanotroughs exhibiting periodic sinusoidal wavy structures. (d) AFM study of a typical buckled Au nanotrough. Inset shows that the heights of the different segments on a single nanotrough are highly consistent.

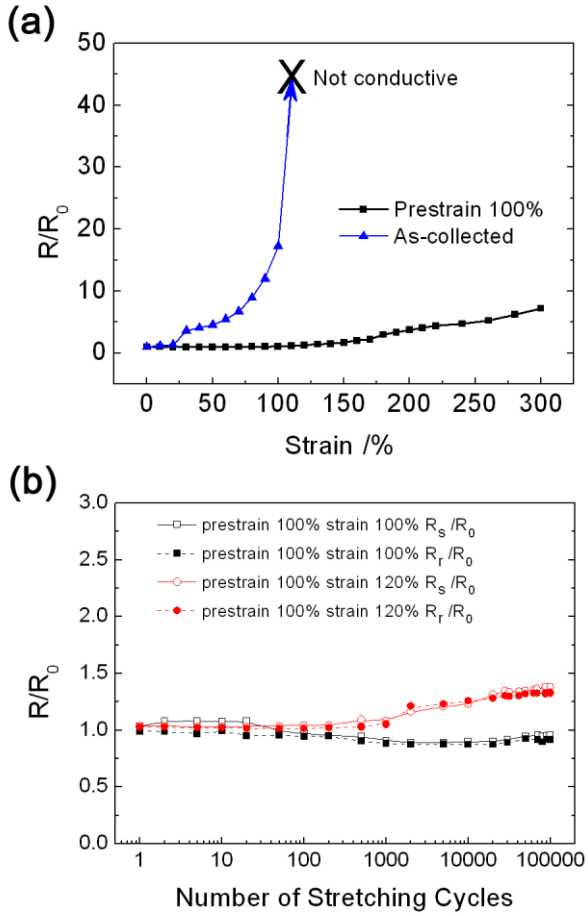

Figure 3. (a) Resistance change of as-collected Au nanotrough and buckled Au nanotrough networks (released from uniaxial pre-strain of 100%) under different tensile strains. (b) Resistance change of buckled Au nanotrough networks (released from uniaxial pre-strain of 100%) under cyclic stretching to 100% and 120% for 100,000 cycles. R_s and R_r are the resistance of the nanotrough film measured under and after releasing of tensile strains, respectively.

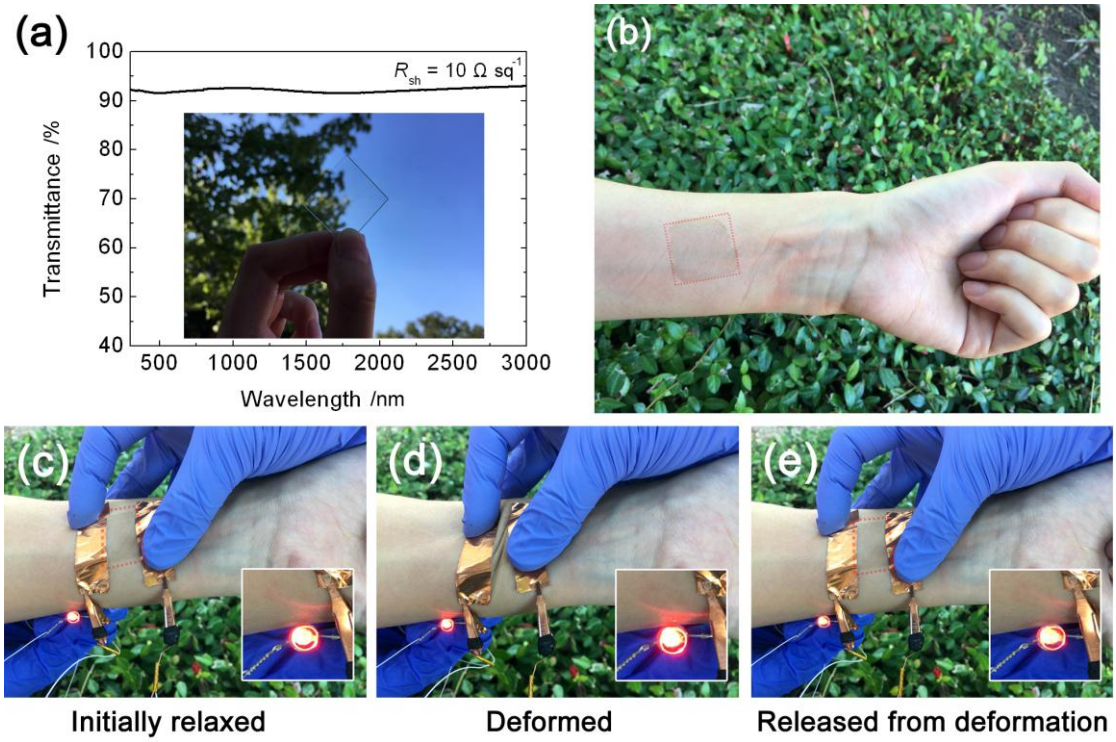

Figure 4. (a) Specular transmittance of Au nanotrough networks. Inset shows a Au nanotrough film transferred on a glass substrate. (b) A Au nanotrough film transferred on human skin. (The sample region is marked by a red dashed square.) (c-e) Demonstration of E-skin devices based on Au nanotrough films. The Au nanotrough film (indicated by dashed lines) was connected in series with a red LED light. The luminance of LED did not change during the whole skin deformation process.

Table 1. Comparison of stretchability and fatigue properties of novel FTE materials

FTE	T @ 550 nm	R_{sh} (Ω sq^{-1})	One-time stretchability	Stretching fatigue
AgNW network (long)[16]	90%	9	R/R_0 ~500 @ 90% strain (with no pre-strain) OR R/R_0 ~5 @ 250% strain (with 125% pre-strain)	—
Conducting-polymer-soldered AgNW network [30]	85%	25	R/R_0 ~12 @ 20% strain	—
GO-soldered AgNW network[31]	88%	14	R/R_0 ~20 @ 100% strain	R/R_0 ~4.8 after 100 cycles @ 40% strain
Spray-coated CNT films[22]	79%	328	R/R_0 ~6 @ 150% strain	Stable after 12,500 cycles @ 25% strain
AgNW-CNT hybrid composite[32]	88%	27	R/R_0 ~8 @ 460% strain (with 150% pre-strain)	—
Au nanotrough network[19]	90%	8	$\Delta R_{sh}/R_0$ ~40% after releasing of 50% strain	—
Au nanomesh[18,33]	82.5%	20	R/R_0 ~3.5 @ 240% strain (with 100% pre-strain)	$\Delta R/R_0$ ~9% after 54,000 cycles @ 100% strain (with 100% pre-strain)
Buckled Au@ PVP nanofiber network[34]	87	79	R/R_0 ~11 @ 70% strain (with 20% uniaxial pre-strain) or R/R_0 ~2.4 @ 140% strain (with 20% biaxial pre-strain)	$\Delta R/R_0$ ~83% after 1,000 cycles @ 60% strain (with 20% biaxial pre-strain)

Buckled Au nanotrough (this work)	91	10	R/R_0 ~7 @ 300% strain (with 100% pre-strain)	No R increase after 100,000 cycles @ 100% strain OR $\Delta R/R_0$ ~38% after 100,000 cycles @ 120% strain (with 100% pre-strain)

Table of Contents

A highly stretchable flexible transparent electrode based on an in-plane buckled Au nanotrough network is engineered, showing excellent stretchability (300% tensile strain) with no fatigue upon cyclic stretching to 100% strain for 100,000 cycles. Combined with its superior optoelectronic performance (R_{sh} ~10 Ω/sq at T = 91%), the Au nanotrough networks can be applied to human skins as flexible electrodes.

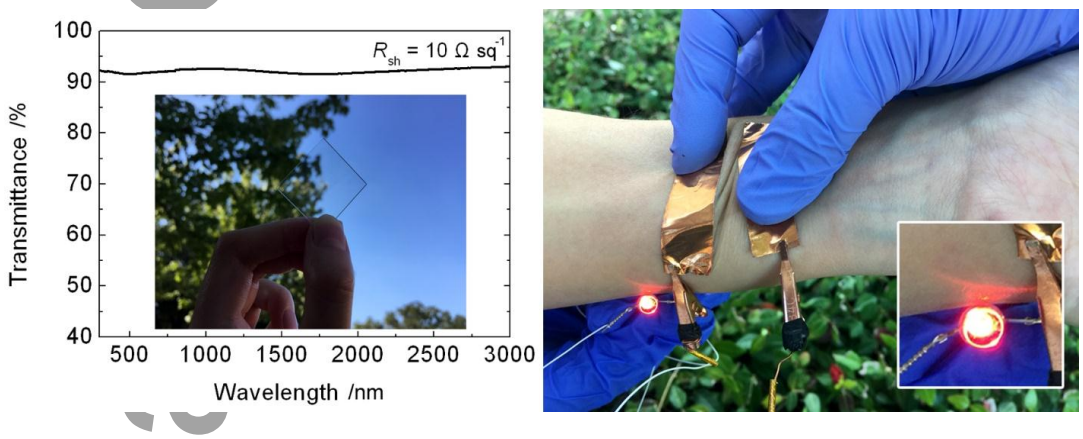

Supporting Information

A Highly Stretchable and Fatigue-free Transparent Electrode Based on an In-plane Buckled Au Nanotrough Network

Siya Huang[1†], *Yuan Liu*[1†], *Chuan Fei Guo*[2*], *and Zhifeng Ren*[1*]

[1] Department of Physics and TcSUH, University of Houston, Houston, Texas 77204, USA

[2] Department of Materials Science and Engineering, South University of Science and Technology of China, Shenzhen, Guangdong 518055, China

[†] These authors contributed equally to this work.

[*] Correspondence to: zren@uh.edu; guocf@sustc.edu.cn

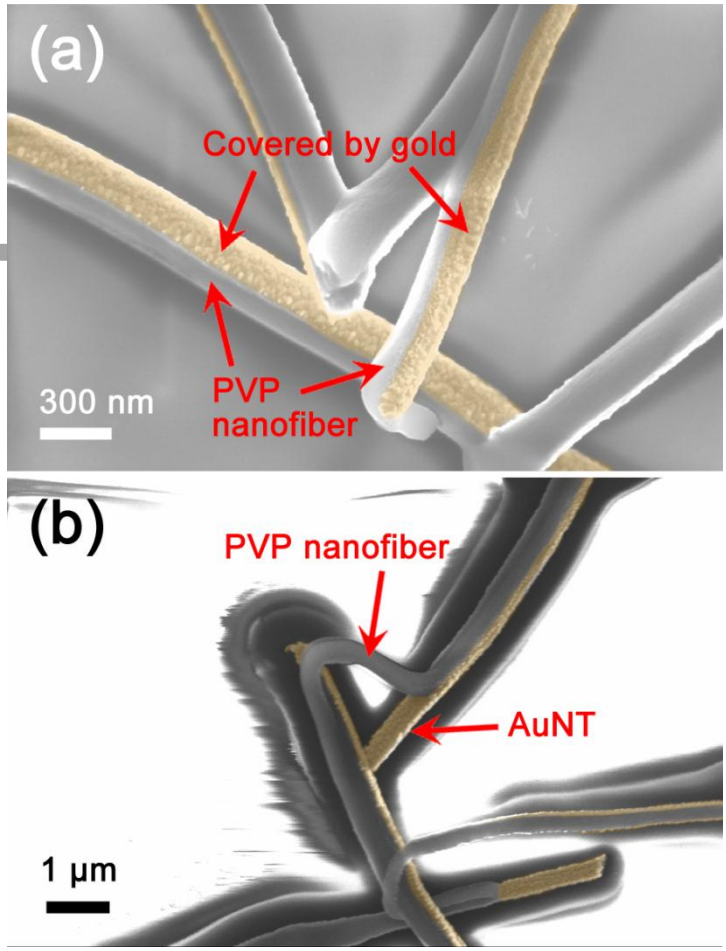

Figure S1. SEM images of PVP nanofibers half coated with Au. (a) A layer of Au film was deposited on the upper side of the PVP nanofibers as marked in yellow. (b) A part of the Au nanotrough has peeled off the PVP nanofiber as indicated by arrows.

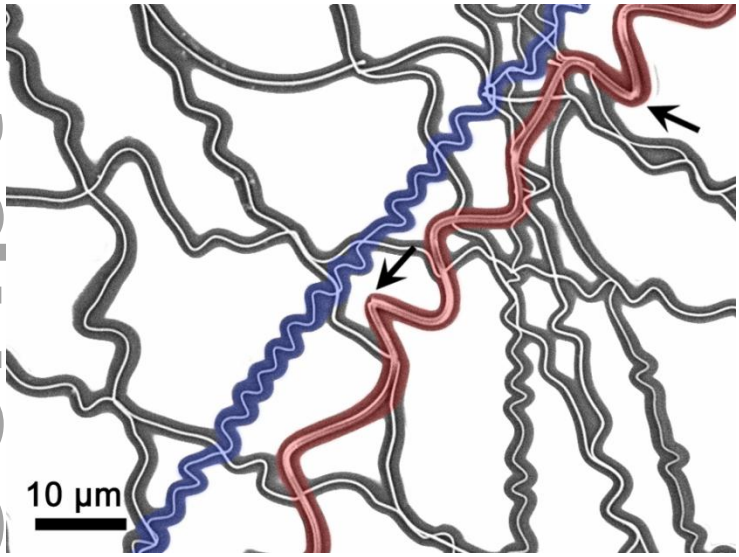

Figure S2. Different deformation modes of Au nanotroughs with different diameters. Upon releasing of pre-strains, the thicker Au nanotrough (marked in red, *d* ~850 nm) did not form sinusoidal wavy structures as the thinner Au nanotrough (marked in blue, *d* ~200 nm). Arrows indicate locations where fractures occur.

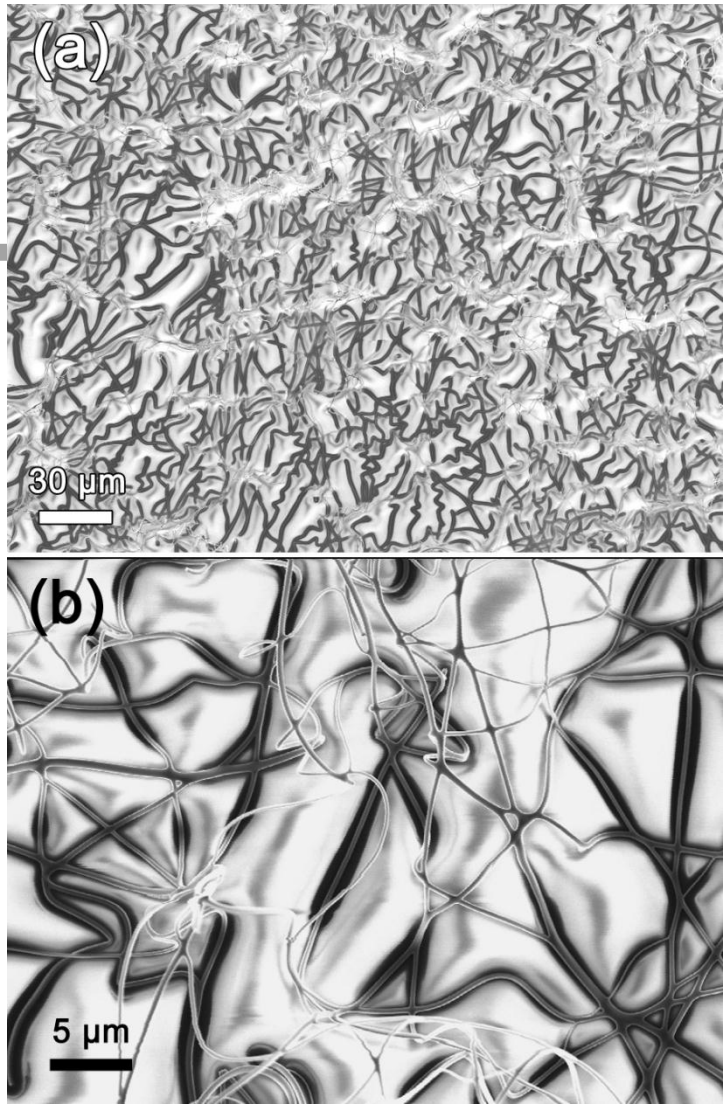

Figure S3. (a) Out-of-plane deformation formed in Au nanotrough networks with smaller pore sizes upon releasing from pre-strains. (b) Magnified SEM image of the out-of-plane deformation.